Supporting Information

Regulation of the Adsorption Site of Ni_2P by Ru and S Co-doping for Ultra-efficient Alkaline Hydrogen Evolution

Xiaodeng Wang[a,b,c], Qi Hu[a], Guodong Li[a], Shaomin Wei[a], Hengpan Yang[a], Chuanxin He[a],*

[a] College of Chemistry and Environmental Engineering, Shenzhen University, Shenzhen, 518060, China
[b] Key Laboratory of Optoelectronic Devices and Systems of Ministry of Education and Guangdong Province, College of Optoelectronic Engineering, Shenzhen University, Shenzhen, 518060, China
[c] Department of Chemistry and Environmental Engineering, Hanshan Normal University, Qiaodong, Chaozhou, China

ECSA and TOF

The electrochemical active surface area (ECSA) was estimated using the capacitance (Cdl) by the following equation, where the specific capacitance for a flat surface is used as 40 μF cm^{-2} as reported.

$$A_{ECSA}^{NiP2} = \frac{C_{dl}}{40\ \mu F\ cm^{-2}\ per\ cm^2}$$

To calculate the per-site turnover frequency (TOF), we used the following formula:

$$\text{TOF} = \frac{\#total\ hydrogen\ turn\ overs\ /\ cm^2\ geometric\ area}{\#surface\ sites\ /\ cm^2\ geometric\ area}$$

The total number of hydrogen turn overs was calculated from the current density according to :

$$\#_{H2} = \left(j\ \frac{mA}{cm^2}\right)\left(\frac{1\ C\ s^{-1}}{1000mA}\right)\left(\frac{1\ mol\ e^-}{96485.3\ C}\right)\left(\frac{1\ mol\ H_2}{2\ mol\ e^-}\right)\left(\frac{6.022 \times 10^{23} H_2\ molecules}{1\ mol\ H_2}\right)$$

$$= 3.12 \times 10^{15} \frac{H_2/s}{cm^2}\ per\ \frac{mA}{cm^2} \times |j|$$

#surface sites per real surface area:

For Ni_2P

$$\#surface\ sites = \left(\frac{3\ atoms/unit}{100.0397\ Å^3/unit}\right)^{\frac{2}{3}}$$

$$= 0.9654 \times 10^{14} atoms\ cm^{-2}$$

Finally, plot of current density can be converted into a TOF plot according to

$$\text{TOF} = \frac{3.12 \times 10^{15} \frac{H_2/s}{cm^2}\ per\ \frac{mA}{cm^2} \times |j|}{\#surface\ sites \times A_{ECSA}^{NiP2}}$$

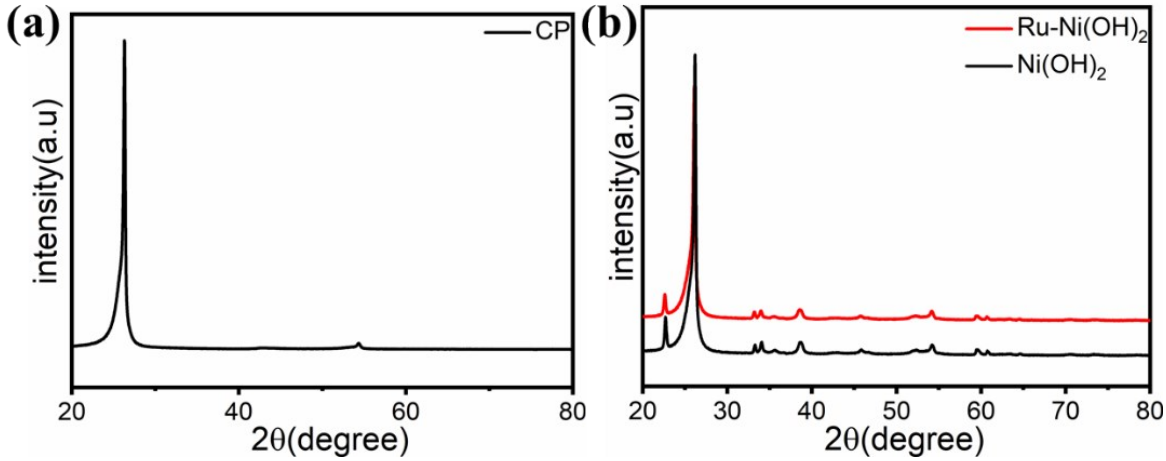

Figure S1 XRD patterns for (a) CP and (b) Ru-$Ni(OH)_2$ and $Ni(OH)_2$.

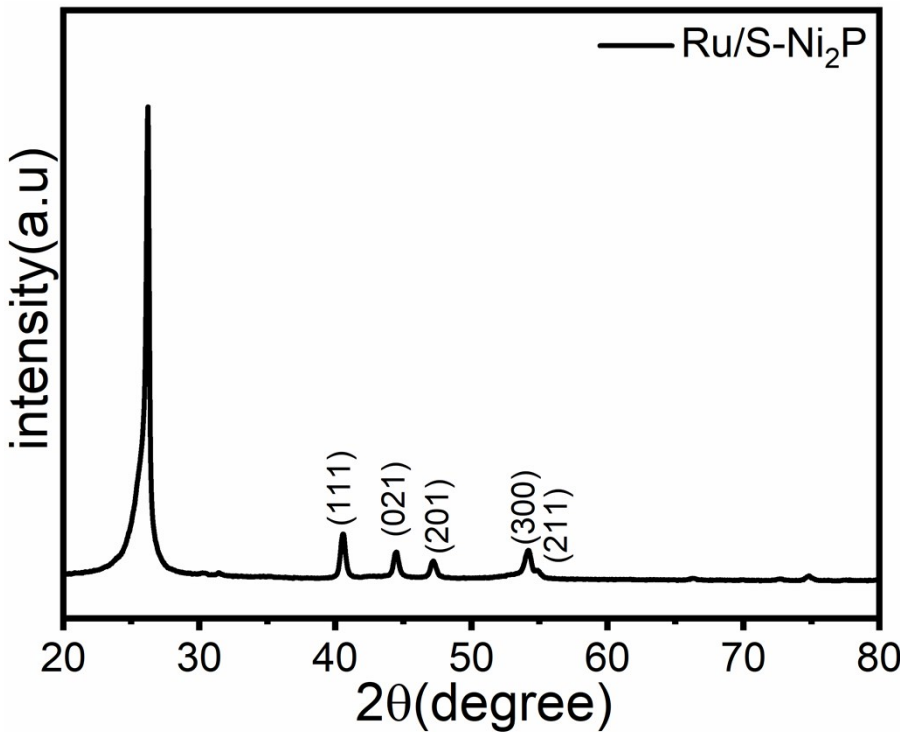

Figure S2 XRD for Ru/S-Ni_2P.

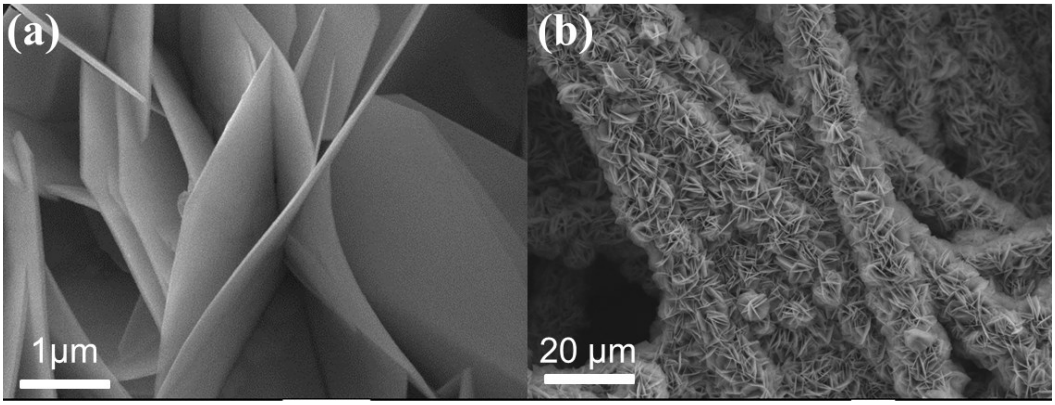

Figure S3 SEM images for (a) $Ni(OH)_2$ and Large-scale SEM images for (b) $Ni(OH)_2$.

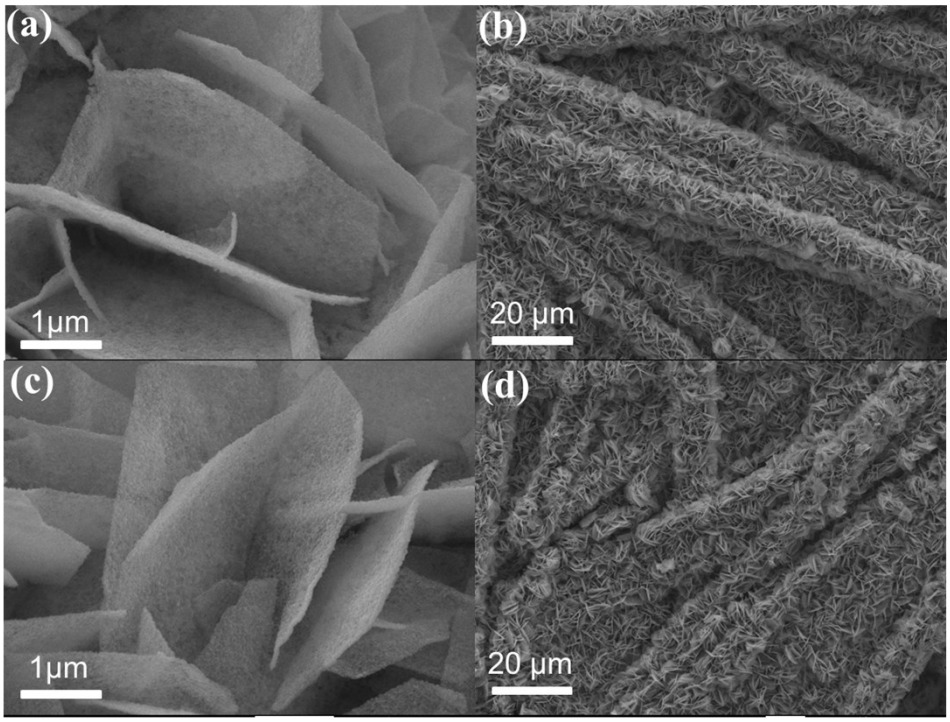

Figure S4 SEM images for (a) Ni_2P, (c) S-Ni_2P. Large-scale SEM images for (b) Ni_2P and (d) S-Ni_2P.

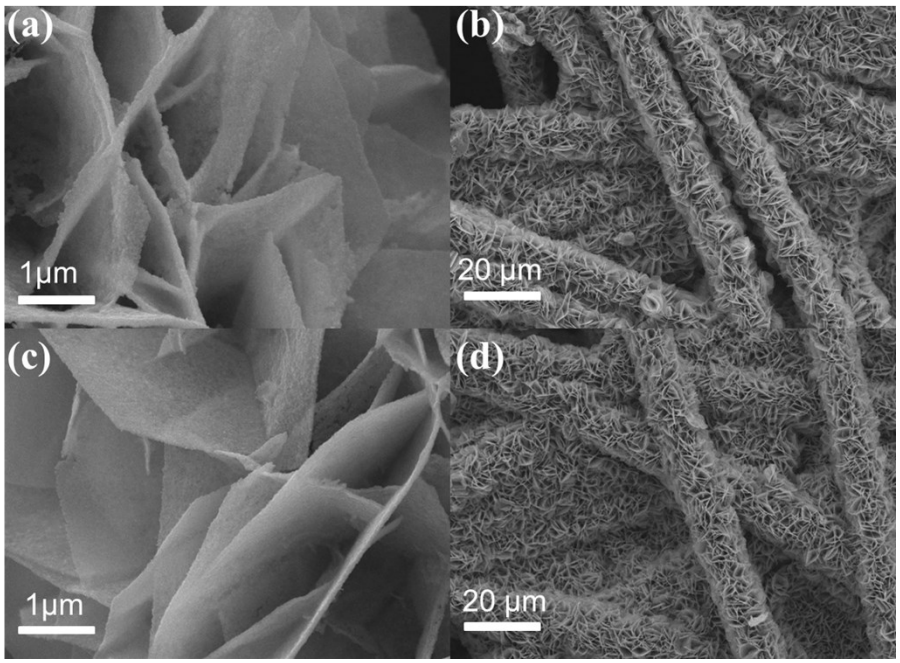

Figure S5 SEM images for (a) Ru-Ni_2P, (c) Ru/S-Ni_2P. Large-scale SEM images for (b) Ru-Ni_2P and (d) Ru/S-Ni_2P.

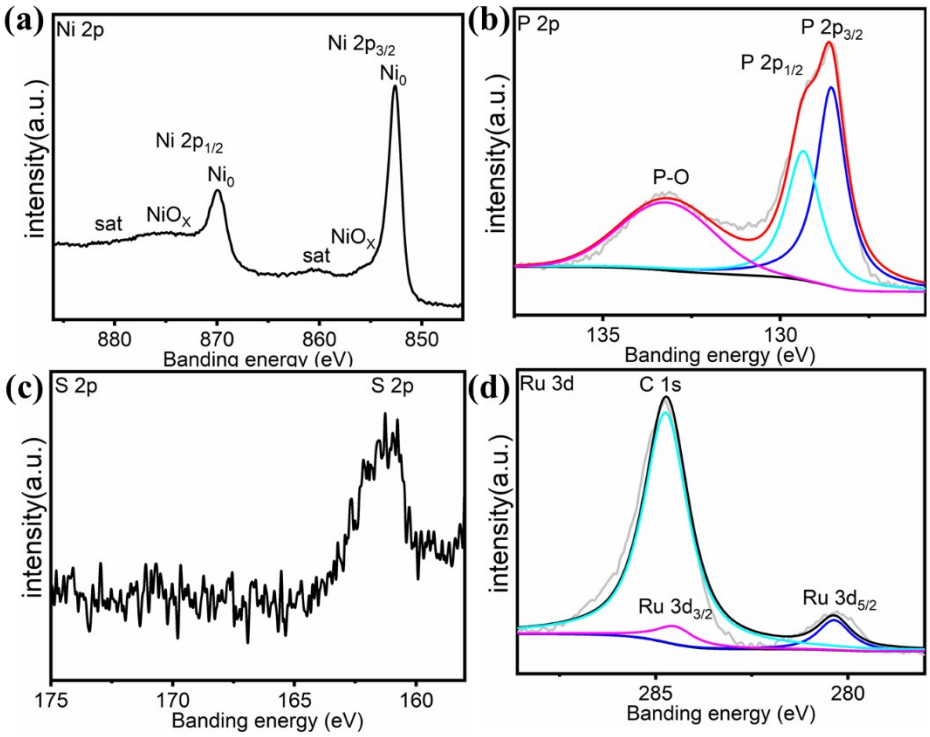

Figure S6 XPS spectra of (a) Ni 2p, (b)P 2p, (c) S 2p and (d) Ru 3d regions for Ru/S-Ni_2P.

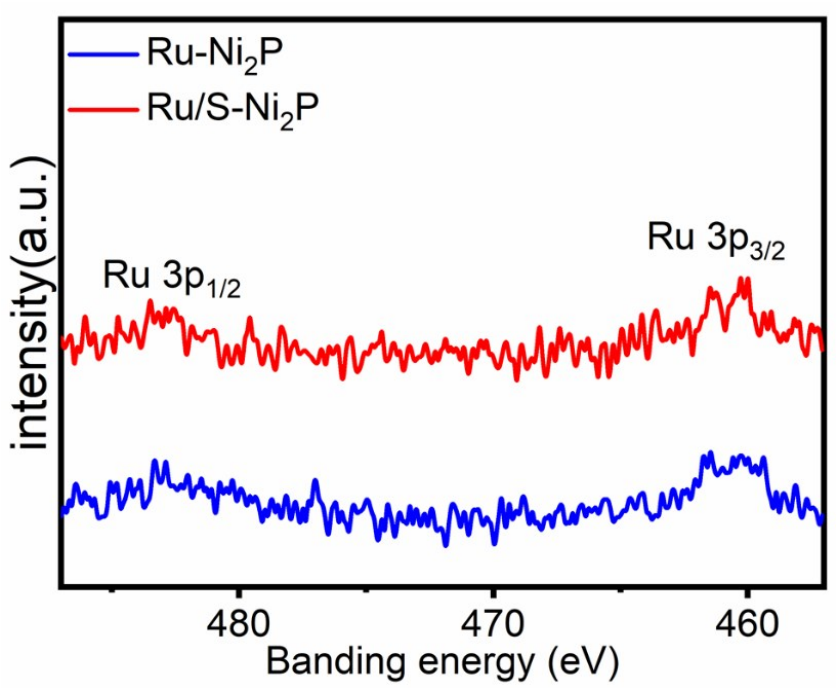

Figure S7 XPS spectra of Ru 3p regions for Ru-Ni_2P and Ru/S-Ni_2P.

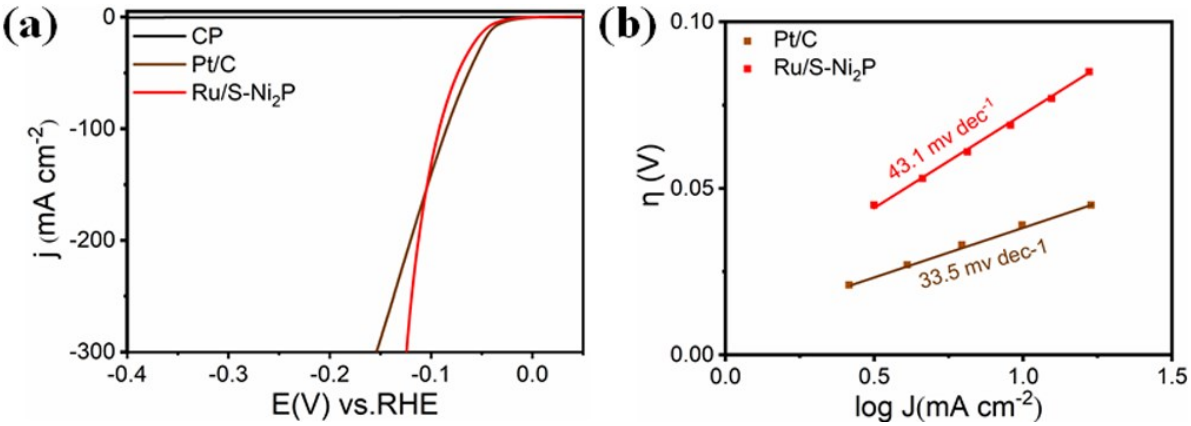

Figure S8 (a) LSV curves of Pt/C and Ru/S-Ni_2P in 1 M KOH. (b) The corresponding Tafel plots.

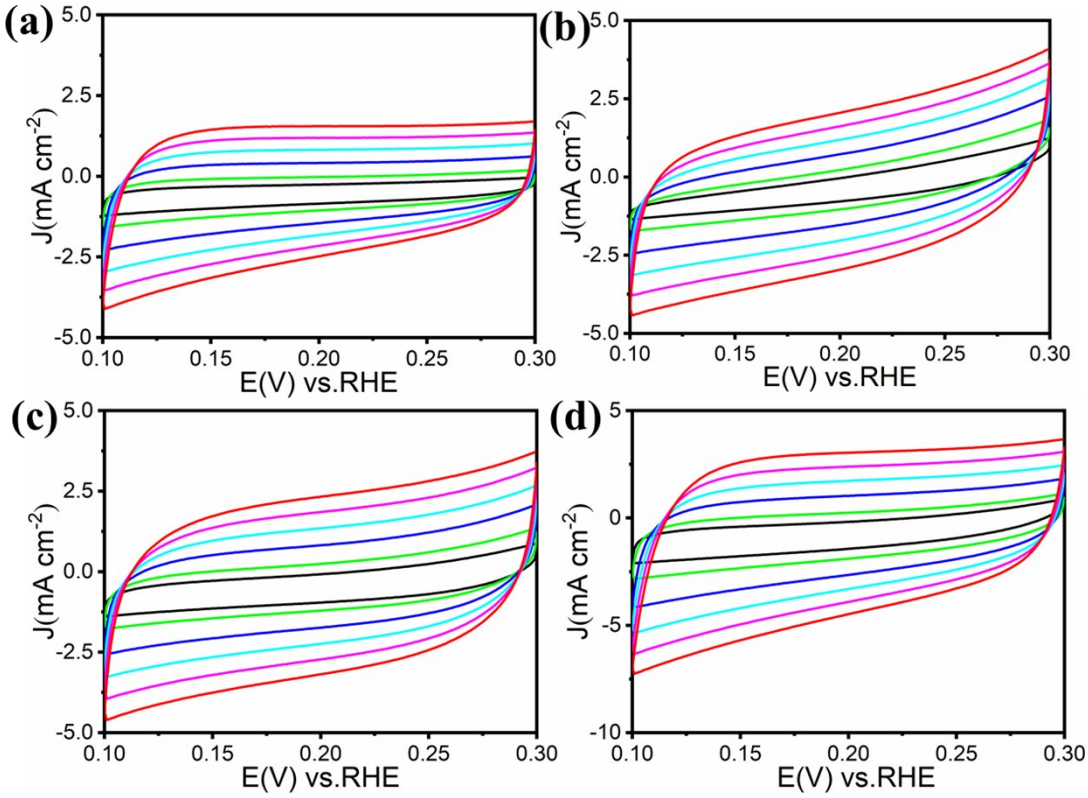

Figure S9 CVs for Ni_2P (a), S-Ni_2P (b), Ru-Ni_2P (c) and Ru/S-Ni_2P (d).

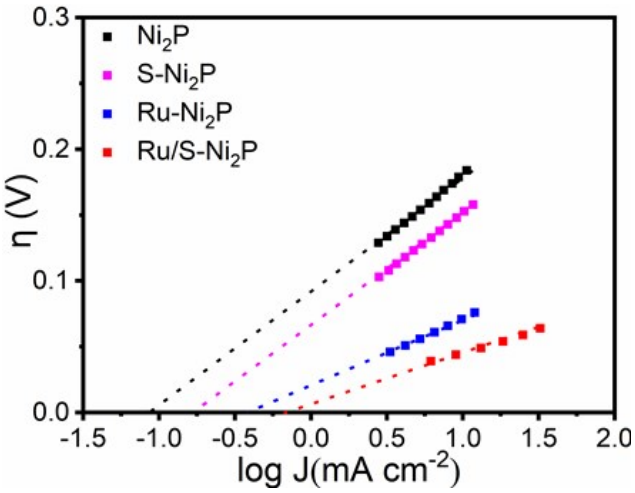

Figure S10 Calculated exchange current density for Ni_2P, S-Ni_2P, Ru-$Ni_2P$and Ru/S-Ni_2P in 1 M KOH by applying extrapolation method to the Tafel plot.

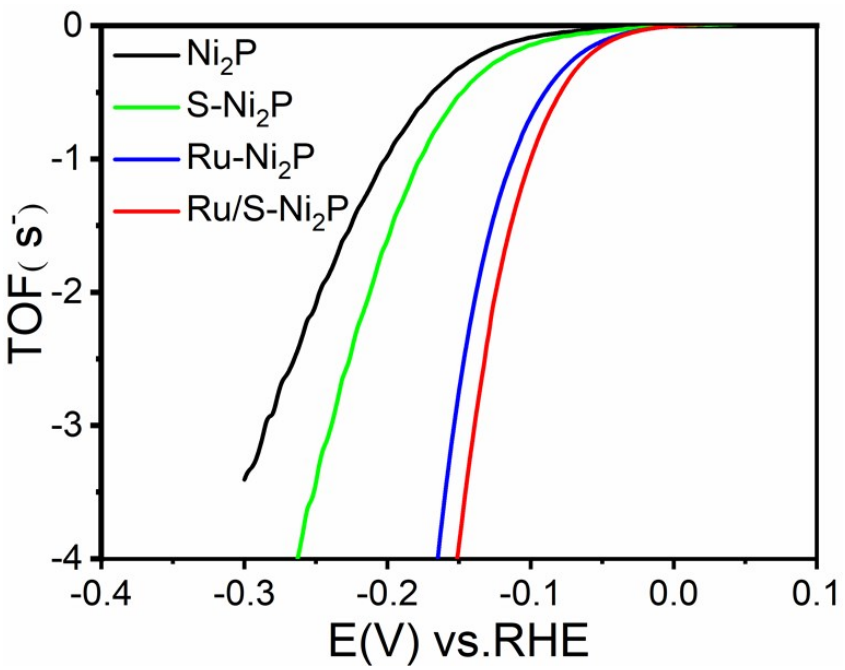

Figure S11 Calculated TOF for Ni_2P, S-Ni_2P, Ru-$Ni_2P$and Ru/S-Ni_2P in 1 M KOH.

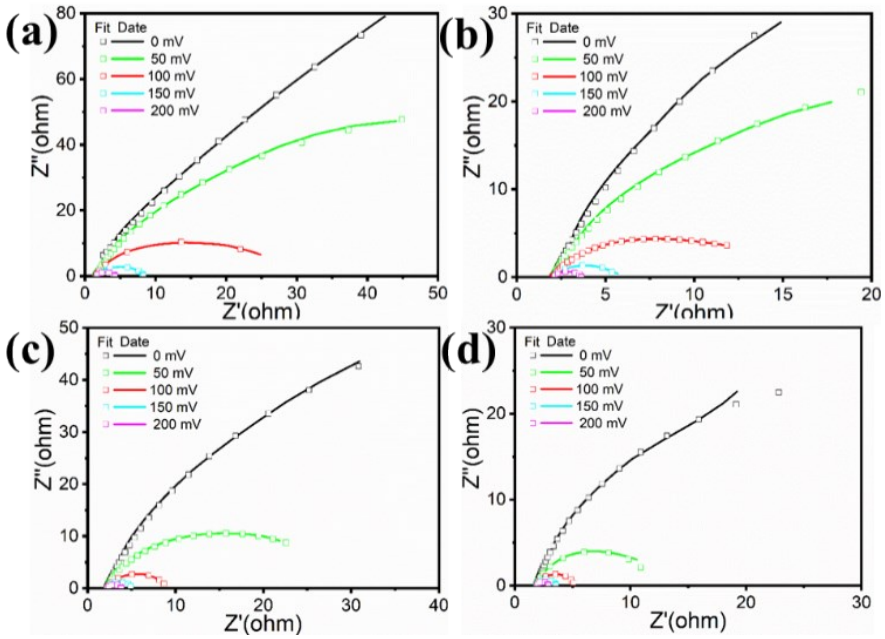

Figure S12 Nyquist plots of Ni_2P (a), S-Ni_2P (b), Ru-Ni_2P (c) and Ru/S-Ni_2P (d)at different overpotential.

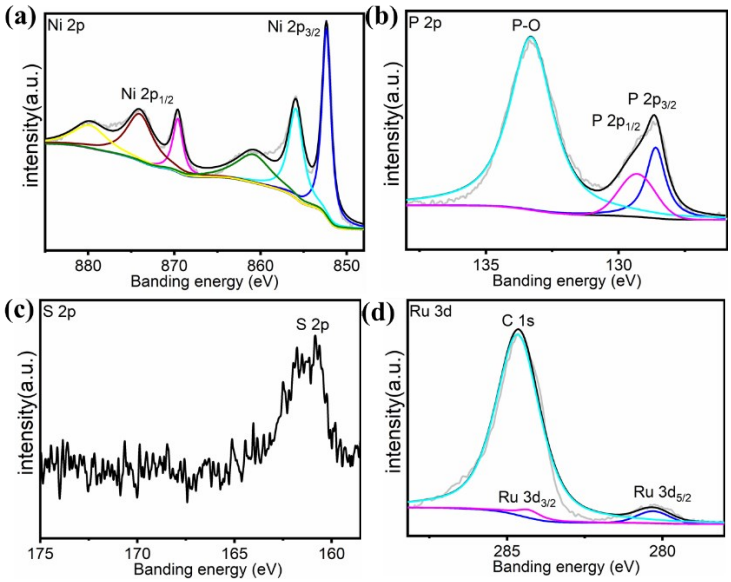

Figure S13. XPS spectra of (a) Ni 2p, (b)P 2p, (c) S 2p and (d) Ru 3d regions for Ru/S-Ni_2P after HER hydrolysis.

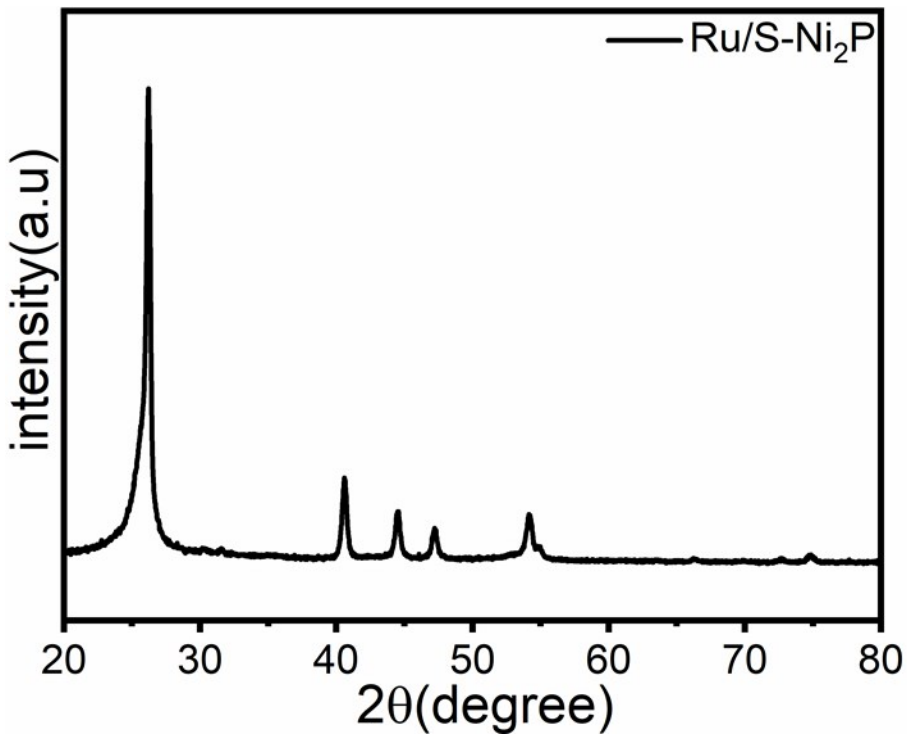

Figure S14 (a) XRD pattern for Ru/S-Ni_2P after HER hydrolysis.

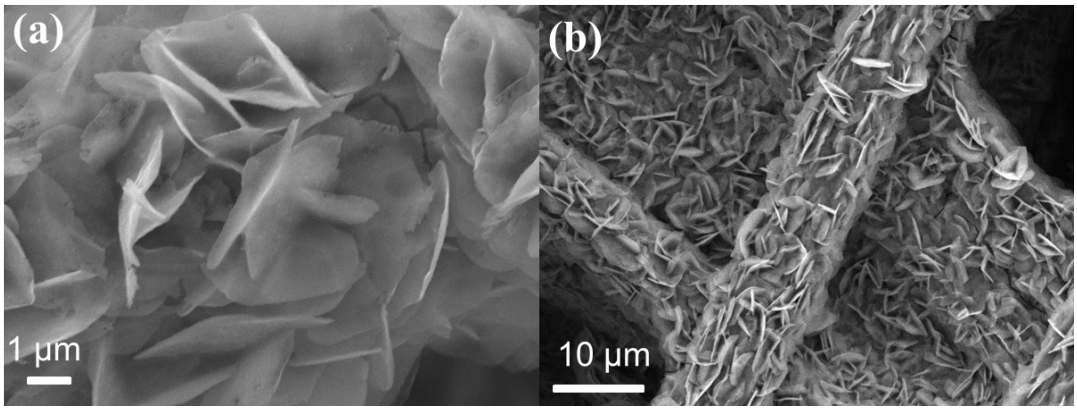

Figure S15. (a) SEM image of the Ru/S-Ni_2P after electrolysis.

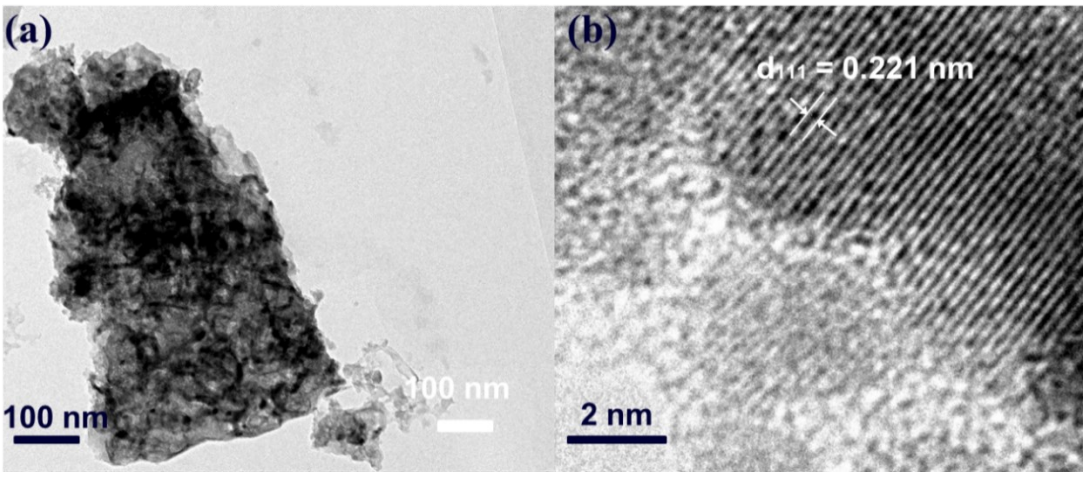

Figure S16. (a) TEM images and (b) lattice image of the Ru/S-Ni_2P after electrolysis.

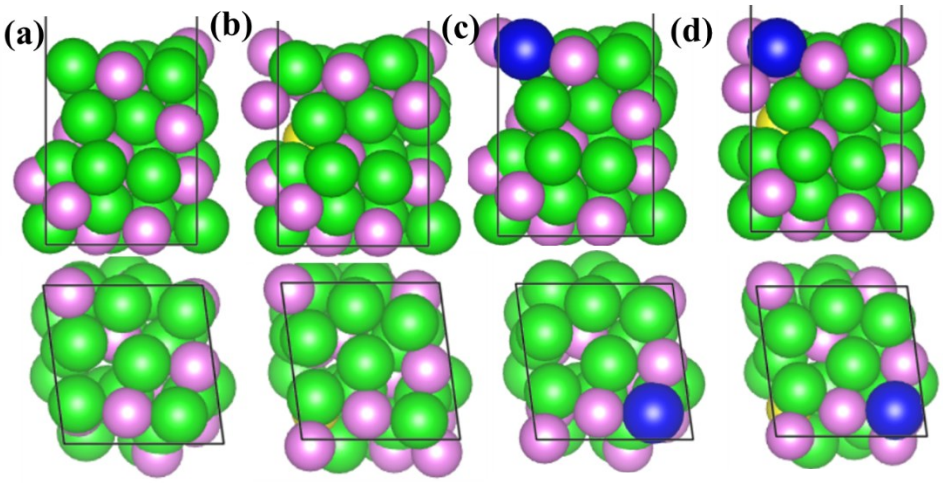

Figure S17. Top and side view of Ni_2P (a), S-Ni_2P (b), Ru-Ni_2P (c) and Ru/S-Ni_2P (d). Green, pink, yellow and blue balls represent Ni, P, S and Ru atoms, respectively.

Table S1 Comparison of HER performance in alkaline media for Ru/S-Ni_2P with other TMs HER electrocatalysts.

Catalysts	J(mA cm^{-2})	η (mV vs RHE)	Tafel Slope (mV dec^{-1})	Ref
Ni_2P /Ni	10	141	68	S1[1]
Ni_2P/Ti	10	120	60	S2[2]
NiP_2 NS/CC	10	75	51	S3[3]
Ni_2P NPs	20	130	81	S4[4]
N-MoP/CC	10	70	55	S5[5]
Mo-Ni_2P	10	81	53.4	S6[6]
Mn−CoP	10	76	52	S7[7]
O, Cu-CoP	10	72	62.6	S8[8]
Ni_2P-$NiSe_2$	10	66	72.6	S9[9]
S-MoP	10	104	56	S10[10]
Ni_3S_2/NF	10	149	127	S11[11]
N, Mn-MoS_2	10	66	50	S12[12]
P/Ni−Mo_2C	10	165	53.6	S13[13]
$Ni_{1.5}Co_{1.4}P$@Ru	10	52	50	S14[14]
Ni@Ni_2P−Ru	10	80	41	S15[15]
S-Co_2P@NCC	10	105	77	S16[16]

S,N-MoP	**10**	**63**	**44**	**S17[17]**
FeP_2/C	**10**	**~150**	**66**	**S18[18]**
Ni-P/Ni/NF	**10**	**129**	**70**	**S19[19]**
Ni_2P–$Ni_{12}P_5$	**10**	**76**	**68**	**S20[20]**
Fe-Ni_2P	**10**	**106**	**37.7**	**S21[21]**
Ru/S-Ni_2P	**10** **50**	**49** **75**	**49.5**	**This work**

Table S2. Summary of the electrochemical properties of Ni_2P, Ru-Ni_2P, S-Ni_2P and Ru/S-Ni_2P. Note that the $J_{0,normalized}$ is normalized by relative surface area (C_{dl}).

Sample	**J_0 (mA/cm^2)**	**C_{dl} (mF/cm^2)**	**Relative surface area**	**$J_{0,normalized}$ (mA/cm^2)**
Ni_2P	**0.095×10^{-3}**	**19.2**	**1**	**0.095×10^{-3}**
S-Ni_2P	**0.178×10^{-3}**	**23.5**	**1.2**	**0.148×10^{-3}**
Ru-Ni_2P	**0.398×10^{-3}**	**25.8**	**1.34**	**0.297×10^{-3}**
Ru/S-Ni_2P	**0.668×10^{-3}**	**34.6**	**1.80**	**0.371×10^{-3}**

Table S3 Summary of the Rct values for Ni_2P, Ru-Ni_2P, S-Ni_2P and Ru/S-Ni_2P at certain overpotential from 0 mV to 200 mV.

Sample	**0 mV (Ω)**	**50 mV (Ω)**	**100 mV (Ω)**	**150 mV (Ω)**	**200 mV (Ω)**
Ni_2P	**611.20**	**139.80**	**26.03**	**6.70**	**1.40**
S-Ni_2P	**171.10**	**63.64**	**11.59**	**3.50**	**1.32**

Ru-Ni_2P	**146.70**	**27.07**	**6.79**	**2.85**	**1.05**
Ru/S-Ni_2P	**60.64**	**10.07**	**3.29**	**1.68**	**1.02**

References

[1] Y. Shi, Y. Xu, S. Zhuo, J. Zhang, B. Zhang, *ACS Appl. Mater. Interfaces* **2015**, 7, 2376.

[2] Z. Pu, Q. Liu, C. Tang, A. M. Asiri, X. Sun, *Nanoscale* **2014**, 6, 11031.

[3] P. Jiang, Q. Liu, X. Sun, *Nanoscale* **2014**, 6, 13440.

[4] E. J. Popczun, J. R. McKone, C. G. Read, A. J. Biacchi, A. M. Wiltrout, N. S. Lewis, R. E. Schaak, *J. Am. Chem. Soc.* **2013**, 135, 9267.

[5] N. Chen, W. Zhang, J. Zeng, L. He, D. Li, Q. Gao, *Appl. Catal. B Environ.* **2020**, 268.

[6] Q. Wang, H. Zhao, F. Li, W. She, X. Wang, L. Xu, H. Jiao, *J. Mater. Chem. A* **2019**, 7, 7636.

[7] T. Liu, X. Ma, D. Liu, S. Hao, G. Du, Y. Ma, A. M. Asiri, X. Sun, L. Chen, *ACS Catal.* **2016**, 7, 98.

[8] K. Xu, Y. Sun, Y. Sun, Y. Zhang, G. Jia, Q. Zhang, L. Gu, S. Li, Y. Li, H. J. Fan, *ACS Energy Lett.* **2018**, 3, 2750.

[9] C. Liu, T. Gong, J. Zhang, X. Zheng, J. Mao, H. Liu, Y. Li, Q. Hao, *Appl. Catal. B Environ.* **2020**, 262.

[10] K. Liang, S. Pakhira, Z. Yang, A. Nijamudheen, L. Ju, M. Wang, C. I. Aguirre-Velez, G. E. Sterbinsky, Y. Du, Z. Feng, J. L. Mendoza-Cortes, Y.

Yang, *ACS Catal.* **2019**, 9, 651.

[11] W. He, L. Han, Q. Hao, X. Zheng, Y. Li, J. Zhang, C. Liu, H. Liu, H. L. Xin, *Acs Energy Lett.* **2019**, 4, 2905.

[12] T. Sun, J. Wang, X. Chi, Y. Lin, Z. Chen, X. Ling, C. Qiu, Y. Xu, L. Song, W. Chen, C. Su, *ACS Catal.* **2018**, 8, 7585.

[13] Z. Li, S. Xu, K. Chu, G. Yao, Y. Xu, P. Niu, Y. Yang, F. Zheng, *Inorg Chem* **2020**, 59, 13741.

[14] S. Liu, Q. Liu, Y. Lv, B. Chen, Q. Zhou, L. Wang, Q. Zheng, C. Che, C. Chen, *Chem. Commun.* **2017**, 53, 13153.

[15] Y. Liu, S. L. Liu, Y. Wang, Q. H. Zhang, L. Gu, S. C. Zhao, D. D. Xu, Y. F. Li, J. C. Bao, Z. H. Dai, *J. Am. Chem. Soc.* **2018**, 140, 2731.

[16] M. A. R. Anjum, M. D. Bhatt, M. H. Lee, J. S. Lee, *Chem Mater* **2018**, 30, 8861-8870.

[17] M. A. R. Anjum, J. S. Lee, *ACS Catal.* **2017**, 7, 3030.

[18] J. Jiang, C. Wang, J. Zhang, W. Wang, X. Zhou, B. Pan, K. Tang, J. Zuo, Q. Yang, *J. Mater. Chem. A* **2015**, 3, 499.

[19] J. Zhang, Z. Zhang, Y. Ji, J. Yang, K. Fan, X. Ma, C. Wang, R. Shu, Y. Chen, *Appl. Catal. B Environ.* **2021**, 282, 119609.

[20] Z. Wang, S. Wang, L. Ma, Y. Guo, J. Sun, N. Zhang, R. Jiang, *Small* **2021**, 17, 2006770

[21] M. Li, J. Wang, X. Guo, J. Li, Y. Huang, S. Geng, Y. Yu, Y. Liu, W. Yang, Appl Surf Sci **2021**, 536, 147909.